ISBN: 978-3-95450-204-2 ISSN: 2673-5350 doi:10.18429/JACoW-IBIC2019-MOPP011

A DUAL FUNCTIONAL CURRENT MONITOR FOR STRIPPING EFFICIENCY MEASUREMENT IN CSNS*

W. L. Huang†, R. Y. Qiu, F. Li, A. X. Wang, M. Y. Liu, M. Y. Huang, T. G. Xu
Institute of High Energy Physics, Chinese Academy of Sciences, Beijing 100049, China
Spallation Neutron Source Science Center, Dongguan 523803, China

Abstract

China Spallation Neutron Source (CSNS), the biggest platform for neutron scattering research in China, has been finished construction and already in user operation stage by the end of 2017. During the multi-turn charge-exchange injection, H- stripping by a carbon primary stripper foil (100 μg/cm^2) and a secondary stripper foil (200 μg/cm^2) is adopted for this high intensity proton synchrotron. In order to evaluate the stripping efficiency and the foil aging, a dual-function low noise current transformer and corresponding electronics are designed to measure the ultra-low intensity of H^- and H^0, which are not stripped completely by the 1st foil but totally stripped charge changing to H^+ and delivered to the IN-DUMP. The self-designed CT sensors made of domestic nano-crystalline toroids, the noise analysis and elimination, measurement results and further improvement proposals are presented in this paper.

INTRODUCTION

As explained in Ref. [1], the beam density in hadron storage rings can be limited at injection by space charge or by the injector capacity. The H^- charge exchange injection technique is adopted to overcome the intensity limitation of the beam emittance increase with the number of injected turns and high losses at the septum. Thus, the multi-turn charge-exchange injection in spallation neutron sources is very common and proved to be effective.

China spallation neutron source (CSNS) consists of an H^- ion source, a 3-MeV RFQ, a 4-tank DTL which accelerates the H^- ions to 80MeV, an 80 MeV to 1.6 GeV RCS and a target station. Main parameters of CSNS are listed in Table 1. During the multi-turn charge-exchange injection, H^- stripping by a carbon primary stripper foil (100 μg/cm^2) and a secondary stripper foil (200 μg/cm^2) is adopted to fulfil a stripping efficiency of > 99.7%. The voltage curves of INBH and INBV magnets are optimized to paint the transverse phase space with a small beam loss [3].

Table 1: Main Parameters of CSNS[2]

Project Phase	I	II
Beam Power on target [kW]	100	500
Proton energy [GeV]	1.6	1.6
Average beam current [μA]	62.5	312.5
Pulse repetition rate [Hz]	25	25
Linac energy [MeV	80	250
Linac type	DTL	+Spoke
Linac RF frequency [MHz]	324	324
Macropulse. ave current [mA]	15	40
Macropulse duty factor	1.0	1.7
RCS circumference [m]	228	228
harmonic number	2	2
RCS Acceptance [πmm-mrad]	540	540
Target Material	Tungsten	Tungsten

In order to evaluate the stripping efficiency and the foil aging, a dual-function low noise current monitor (BCT+FCT) and corresponding electronics are designed to measure the ultra-low intensity of H^- and H^0, which are not stripped completely by the 1st foil but totally stripped charge changing to H^+ and delivered to the IN-DUMP. The layout of the injection region of CSNS is showed in Fig. 1.

BEAM TIME STRUCTURE

The H^- beam in the linac is chopped into micro bunches by a chopper located at the end of LEBT. The chopping factor is adjustable for different operation modes. For example, a chopping factor of 50% is adopted for user mode in normal operation and 75% for single bunch mode in special operation for the back-n experiments, which

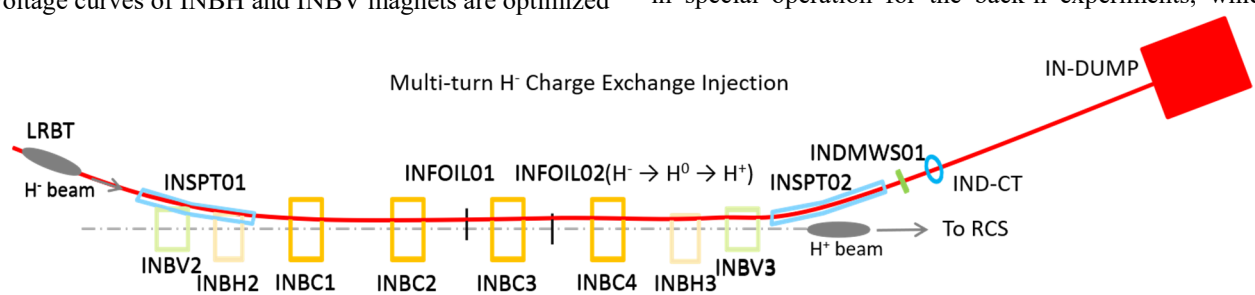

Figure 1: Layout of the injection region of CSNS.

* Work supported by National Natural Science Fund (No.11605214).
† huangwei@ihep.ac.cn

ISBN: 978-3-95450-204-2 ISSN: 2673-5350 doi:10.18429/JACoW-IBIC2019-MOPP011

require a higher time resolution of neutron spectrometers. When the chopped H^- beam are charge-exchange stripped and injected into the RCS ring, the proton beam time structure won't change. Figure 2 shows these two kinds of time structure of the beam.

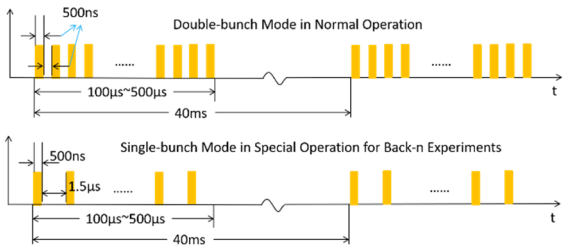

Figure 2: Beam time structures in different operations

There are a BCT(ACCT) and an FCT designed in the beam diagnostics lab of CSNS. The BCT with a low noise electronics is capable to measure the beam intensity as low as 10 μA and the linearity error of the BCT is better than ±1%. According to the beam time structure shown in Fig. 2, the fundamental frequency of the H^+ (proton) beam is 1.022 MHz (double-bunch mode) or 501.1 kHz (single bunch mode). The FCT is required to response to the micro pulse of the stripped beam chain heading to the IN-DUMP of CSNS. The risetime of it should be less than 30 ns, which means the upper-cutting frequency of the FCT bandwidth should be higher than 11.7 MHz. The designed specifications of the BCT and FCT are listed in Table 2.

Table 2: Specifications of BCT and FCT

Specification	BCT	FCT
Range	±50 μA	-
Turns	50	20
τ_{rise}	< 10 μs	< 13.6 ns
Droop	< 1%/ms	< 1%/μs

BCT AND FCT SENSOR OF THE IND-CT

Fabrication

Several kinds of soft magnetic alloy material were tested and compared before the fabrication of current transformers for the IND-CT. Finally, we chose an iron-based soft magnetic alloy core wound with very thin ribbons (20 μm) in high permeability, low loss, and nearly zero magnetostriction, to make the 50-turn BCT(ACCT) and the 20-turn FCT. There is one winding each for the calibration of BCT and FCT. To eliminate the noise from the cable, which is coupled with the power source (INBH and INBV) through the power cables, triax cables are used to transport the sensor signal. There is an extra triax cable casted along with the signal cables for noise measurement, in case the noise from the environment could not be shielded by the shielding layer of the triax cable. We may cancel the noise by the data acquisition system, that is, the sensor signal and the noise are amplified by two same electronics and the noise is cancelled in the data readout and post processing algorithm. Another method is to sample the noise after the electronics with beam off firstly, then subtract the averaged noise from the signal with beam on. The latter one requires only one set of electronics and is now used.

The BCT and FCT sensors were covered with glass tapes for insulation. A short 4-core cable with inner shielding for each two cores was used to link the windings (the secondary winding and the calibration winding) to the triax adapter installed on the outer magnetic shielding. There is similar links using 50Ω coaxial cables for the FCT. Figure 3 showed the self-made BCT and FCT.

Figure 3: A 50-turn BCT and a 20-turn FCT fabricated in the BI lab of CSNS.

The BCT and FCT sensors were placed side by side in the two-layer DT4 shielding with a thin DT4 ring to isolate them. There are two lays of copper sheet with a sheet of polymide between them to form a capacitor just over the ceramic ring, which acts as a LP filter for the sensors. Figure 4 gives the mechanical drawing of the instrumentation.

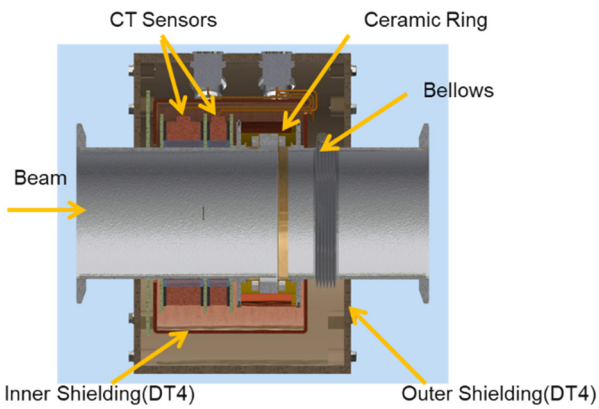

Figure 4: CT sensors and the 2-layer magnetic shielding for the IND-CT in CSNS.

Electronics of BCT and FCT

The output of the BCT electronics is ±10V for the full range 50 μA measurement. A low noise OP is adopted in the circuit since the voltage amplification factor is about 5×10^6 (~134dB). Figure 5 is the schematic of the BCT electronics. For the FCT, a commercial RF pre-amplifier is placed at the cable tunnel just under the accelerator tunnel, very near to the IND-CT. The output signals of the BCT and FCT will be sampled by an NI PXIe-5172 digitizer (100MHz, 8-ch, 14bit ADC and 250MSa/s).

ISBN: 978-3-95450-204-2 ISSN: 2673-5350 doi:10.18429/JACoW-IBIC2019-MOPP011

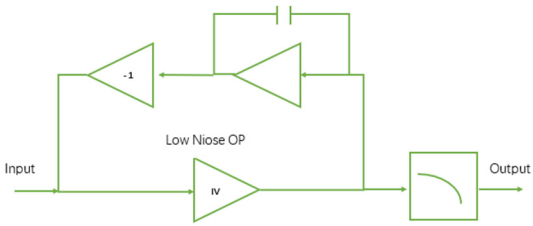

Figure 5: Electronics of the BCT.

Tests in the Lab

The risetime and droop of the BCT with electronics and a 20m-long cable were measured in the beam diagnostics lab with the R&S RTO2004 oscilloscope. The risetime is 5.24 μs (< 10 μs) and the droop is 0.6%/ms (< 1%/ms), which are shown in Fig. 6 and Fig. 7.

Figure 6: Rising time measurement of the BCT.

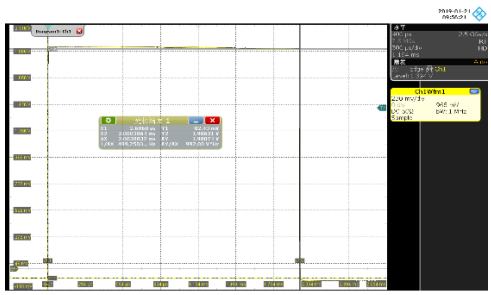

Figure 7: Droop time measurement of the BCT.

To calibrate the BCT and electronics, a pulse current source of KEITHLEY 6221 was used to generate the ultralow current from 10μA to 50μA. The linearity error is with ±1%, given by Fig. 8.

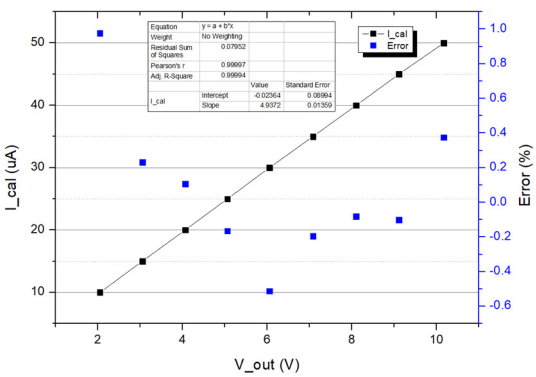

Figure 8: Calibration of the BCT and electronics.

The amplitude frequency response of the FCT was measured using an RF generator (SRS SG382) and the oscilloscope RTO2004. The bandwidth is 550 Hz ~ 375 MHz, showed in Fig. 9.

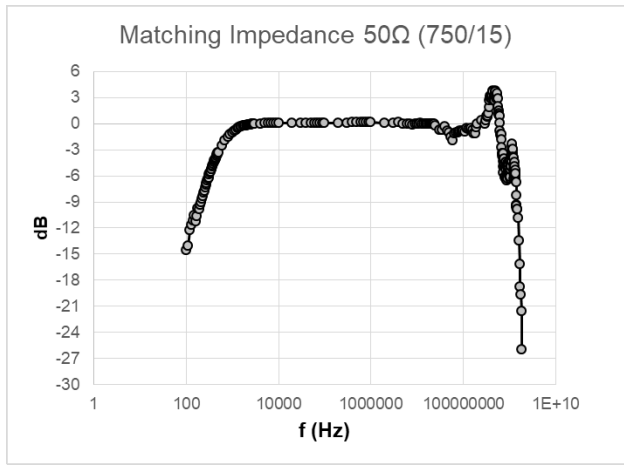

Figure 9: Amplitude frequency response of the FCT.

Tests with Beam On

The dual functional current monitor was installed at the injection region in the accelerator tunnel during this summer maintenance. The DAQ system consists of an NI PXIe-5172 digitizer (100MHz, 8-CH, 14bit ADC and 125MSa/s) and an NI PXI-6358 card for different algorithms of data post processing.

We started the machine study at the beginning of September. When the beam was operated in the Ring-Dump mode, the BCT measured the protons flying towards the IN-Dump successfully. Figure 10 showed the waveform of the 1.2 μA protons with a pulse width of 350 μs. The stripping efficiency could be deduced by the measurement of LRCT03.

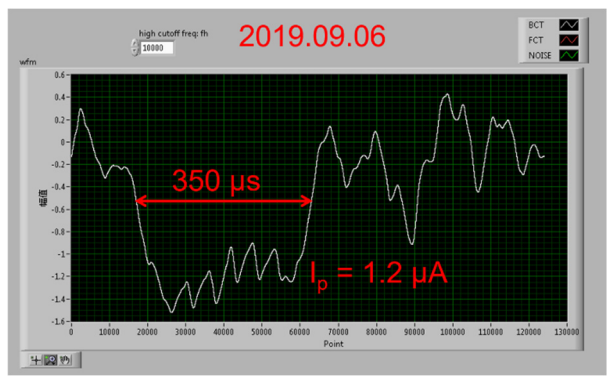

Figure 10: Beam intensity ($H^0 \rightarrow H^+$) measured by BCT.

CONCLUSION

According to the beam time structure and intensity after the second stripping foil, we designed a dual functional current monitor for the stripping efficiency measurement and fabricated the monitor domestically. All the specifications were measured in the lab and passed the acceptance. The IND-CT was tested with beam on during this ma-

ISBN: 978-3-95450-204-2 ISSN: 2673-5350 doi:10.18429/JACoW-IBIC2019-MOPP011

chine study and the noise was eliminated by grounding the triax cable outer shielding at the sensor side and no grounding at the electronics side. The measurement sounds reasonable and need more measurement to test with the stripping foil simulation. An FFT algorithm of the FCT readout, which comes from Ref. [4] will be tested in the further system commissioning.

REFERENCES

[1] C. Bracco, "Phase Space Painting and H- Stripping Injection". in *CERN Yellow Reports: School Proceedings*, [S.l.], v. 5, p. 141, 2018. ISSN 2519-805X.
doi:10.23730/CYRSP-2018-005.141

[2] S. Fu and S. Wang, "Operation Status and Upgrade of CSNS", in *Proc. 10th Int. Particle Accelerator Conf. (IPAC'19)*, Melbourne, Australia, May 2019, pp. 23-27.
doi:10.18429/JACoW-IPAC2019-MOZPLM1

[3] M. Y. Huang, S. Wang, and S. Y. Xu, "Beam Loss and the Stripping Efficiency Measurement for CSNS Injection System", in *Proc. 10th Int. Particle Accelerator Conf. (IPAC'19)*, Melbourne, Australia, May 2019, pp. 2329-2331.
doi:10.18429/JACoW-IPAC2019-WEPMP012

[4] P. K. Saha, et al., "State of the art online monitoring system for the waste beam in the rapid cycling synchrotron of the Japan Proton Accelerator Research Complex", *Phys. Rev. ST Accel. Beams*, vol. 14, Issue 7, 2011.
doi:10.1103/PhysRevSTAB.14.119902